Electronic supplementary information (ESI)

Free carbonate-based molecules in the electrolyte leading to severe safety concern of Ni-rich Li-ion batteries

Experimental section

Synthesis of piperidinium bis(trifluoromethyl sulfonyl)imide (PIPTFSI) with different alkyl chains

The synthesis of ionic liquids is generally composed of 2 steps [1]. The first step is the cation formation. 0.12 mmol of N-methyl piperidine (14.5 mL) was dissolved in acetonitrile. The different alkyl chain lengths including propyl, butyl and pentyl were introduced to cation the structure by adding 0.12 mole of 1-bromopropane (16.4 mL), 1-bromobutane (19.4 mL) and 1-bromopentane (22.3 mL) into the solutions. The solutions were refluxed at 100 °C for overnight. The mixtures were purified by washing with diethyl ether (DE). The second step is a metathesis reaction. Piperidinium-based bromide was dissolved in deionized (DI) water then 29 g (0.10 mol) of lithium bis(trifluoromethanesulfonyl)imide (LiTFSI) were added into the solution. When the reactions finished, 2 layers of aqueous and organic layers were obtained. The organic layers were washed with DI water to remove the residual reactants checked by no precipitants after adding aqueous silver nitrate ($AgNO_3$) into the rinsed water. The synthetic ionic liquids were dried under vacuum at 100 °C for overnight and kept in Ar-filled glove box. The chemical structures of ionic liquids were characterized by ^{1}H, ^{13}C Nuclear Magnetic Resonance (^{1}H and ^{13}C NMR) (Bruker, ascent 600) and atmospheric pressure chemical ionization (APCI) mass spectrometer (Compact QTOF, Bruker).

Physicochemical characterizations

Thermal stability and density of ionic liquids

Thermal stability of synthetic ionic liquids was studied by thermalgravimetric analysis (TGA) (Linseis, STA PT 1600). The samples were heated under nitrogen atmosphere from room temperature to 600 °C in alumina cup with heating rate of 10 ˚C/min and gas flow rate of 100 ml/min. The onset temperature was chosen to indicate the decomposition temperatures of the ionic liquids. The densities of ionic liquids were measured by the pycnometer (AccuPyc II 1345, Micrometritics).

Electrochemical evaluation and conductivity measurement of ionic liquids

The electrochemical stability cell potential windows of ionic liquids were determined by the cyclic voltammetry (CV) using a three-electrode system equipped with Autolab PGSTAT302N (Metrohm). Glassy carbon as a working electrode, platinum rod as counter electrode and printed-screen Ag/AgCl as a reference electrode were used at a scan rate of 10 mV/S. Conductivities of ionic liquids were evaluated by the electrochemical impedance spectroscopy (EIS) measurement of symmetric SS | SS CR2032 coin cells in the frequency range of 500 to 100k Hz and with an amplitude of 10 mV. Bulk resistances were obtained by fitting Nyquist plots with an equivalent circuit to obtain conductivities.

NMR, Mass spectrometry, and TGA

The chemical structures of as-synthesised ILs were confirmed by ^{1}H and ^{13}C NMR techniques. Both ^{1}H and ^{13}C NMR spectra (see **Fig. S1** and **2**) present the successful synthesis of ILs. The purities of ILs were determined by APCI mass spectrometry. From the mass spectra (**Fig. S3A-F**), the molecular peaks of 142.16, 156.15, 170.17 and 279.88 m/z which are relative to the molecular weights of C3-PIP, C4-PIP, C5-PIP cations and TFSI anions are observed. Other molecular peaks besides the cation and anion molecules are not observed indicating high purity of the ILs. Thermal stability which is a remarkable trait of ILs was also evaluated by thermogravimetric analysis (TGA). TGA curves of C3-PIPTFSI, C4-PIPTFSI and C5-PIPTFSI (**Fig. S4**) also show the onset temperature defined as a decomposition temperature of 440 °C, which is the carbonization of carbon containing compounds[2]. Densities of C3-PIPTFSI, C4-PIPTFSI and C5-PIPTFSI are 1.40, 1.37 and 1.34 $\mathrm{gcm^{-3}}$, respectively. Decreasing of densities accompanies with longer alkyl chain on the cations [3, 4].

In situ Differential Electrochemical Mass Spectrometry (DEMS) measurement

In situ gas analysis was carried out using HPR-40 DEMS (Hiden analytical, UK) with QGA professional software. An electron energy of 70 eV was used for ionization of all species, with an emission current of 500 μA. The working pressure was $< 5 \times 10 - 8$ Torr. An 18650 cell without case was used. The fabrication of 18650 jelly roll lithium-ion cell was discussed in the section below. The measurement is performed in an Ar-filled glovebox. The charge-discharge step formation process began at an open circuit potential after 15 min of background measurement.

Fabrication of 18650 lithium-ion cells

All the battery process was carried out in a dehumidifier system with dew point temperature of -40 and -55 °C (for electrolyte injection). The NCA ($LiNi_{0.88}Co_{0.09}Al_{0.03}O_2$, Brunauer–Emmett–Teller surface area ~0.3 m^2g^{-1}, Gelon Corp.) and natural graphite (Gelon Corp.) powdery samples were dried in a vacuum oven at 80 °C for 24 h before used. The slurry of NCA cathode was prepared by mixing of active material, carbon black, and PVDF binder in a weight ratio of 95.2:2.4:2.4 wt.% in NMP (ca. 67.6% solid content) and stirred for 12 h using a vacuum planetary mixer (MTI Corp.) with a cooling system to keep temperature lower than 30 °C. For the graphite anode, the slurry contained 96.6:1.7:1.7 wt.% of graphite, carbon black, and CMC/SBR dispersed in water (ca. 49.3% solid content). Then, the homogeneous slurry was coated using a roll-to-roll automatic coating machine with a built-in dryer (MTI Corp.) at 120 °C and a casting speed of 0.2 m/min. The thickness of cathode and anode was controlled at *ca.* 228 and 240 µm, respectively. The mass loadings of cathode and anode were *ca.* 23.85 mg cm^{-2} and 11.92 mg cm^{-2}, respectively.

The commercial carbonate electrolyte used for the NCA/Graphite LIB is EJN01 consisting of 1 M $LiPF_6$ in EC:DMC:EMC (1:1:1, v/v) with some additives (Gelon LIB group, China). 50% varied-alkyl chain ionic liquids including C3-PIPTFSI, C4-PIPTFSI and C5-PIPTFSI were mixed with the carbonate-based solvents to prepare 1 M $LiPF_6$. All electrolyte preparation was carried out in the glovebox inside the dry room with a dew point temperature of -55 °C.

The 18650 LIB cells of NCA and graphite electrodes were assembled with separator of tri-layer (PP/PE/PP) film. 5 g of the as-prepared electrolyte were injected to each cell. The NCA/Graphite 18650 cells were aged at room temperature for 24 h before the performance evaluation of LIBs. Then, the formation protocol was applied with a step current starting with 0.04C, 0.06C, 0.08C, and 0.1C for 1 cycle at 4.2−3.0 V and 0.02C (1C = 1800 mA).

Electrochemical evaluation of NCA/Graphite 18650 cylindrical cells and safety test

The fabricated NCA/Graphite 18650 cells with the hybrid electrolyte were electrochemically evaluated by the 18650-cell battery tester (Gelon LIB group, China). The first step is the standard charging protocol for LIB cells, which is constant current constant voltage (CCCV) before the evaluation. After that, the capacity of NCA/Graphite 18650 cells was determined at 0.1C and then the cycling ability was tested at 0.5C. Flammability of hybrid electrolytes was tested using the CR 2032-coin case containing 500 µL of hybrid electrolytes. The samples were ignited by using butane blow torch flame. The explosion test of NCA/Graphite 18650 cells was tested by the impact test (UN38.3). The cells were fully charged up to 4.2 V and put in the safety test box equipped with 9.2 kg stainless steel (316 bar). The stainless-steel bar was dropped to the fully charged cells from the height of 610 cm by following the standard of UN 38.3.

Classical molecular dynamic (MD) simulation details

The classical molecular dynamics (MD) simulations were developed by the optimized potentials for liquid simulations for all-atom (OPLS-AA)[5-8] force field methods for the bond relations (bonds, angles, dihedrals, and impropers). The partial atomic charges for all molecules were obtained by optimizing the geometry using Becke's three parameter exchange function combined with the Lee–Yang–Parr correlation functional (B3LYP)[9] based on the density functional theory (DFT) with the aug-cc-pvdz basis set using the Gaussian 16 simulation package.[10] After that, the electrostatic potential surface was fitted by the RESP[11, 12] method. The simulation cubic boxes were constructed with randomly placed 52 Li^+, 52 PF_6^- using PACKMOL[13]. The final concentration of the solution systems is 1.0M lithium salt. The system was equilibrated in a cubic box with periodicity in x, y, and z directions. The initial configuration was energy minimized with a conjugate gradient algorithm for 20,000 steps. By following the minimization, the system was equilibrated with the isothermal-isobaric ensemble at constant number of particles N, pressure P, and temperature T (NPT) for 0.5 ns with a time step of 0.5 fs and the temperature of 298 K. For production runs, 2 ns simulations at 300 K were carried out in the constant number of particles N, volume V, and temperature T (NVT) with the Nosé-Hoover chain (NHC)[14] thermostat with a time step of 1 fs and the temperature of 298 K. The last 0.5 ns of the production runs were used for the MD analysis in this publication. All classical MD simulations were performed with the GROMACS[15-20] simulation package on a 16-cores Unix-based cluster.

Supporting results

^{1}H NMR spectra

C3-PIPTFSI (δ/ppm): 0.98 ($\mathrm{C\underline{H}_3CH_2CH_2}$), 1.74 ($\mathrm{CH_3C\underline{H}_2CH_2}$), 1.86 ($\mathrm{CH_2C\underline{H}_2CH_2}$), 2.98 ($\mathrm{C\underline{H}_3N^+}$), 3.21 ($\mathrm{CH_2C\underline{H}_2N^+}$)

C4-PIPTFSI (δ/ppm): 1.00 ($\mathrm{C\underline{H}_3CH_2CH_2}$), 1.43 ($\mathrm{CH_3C\underline{H}_2CH_2}$), 1.72 ($\mathrm{CH_2C\underline{H}_2CH_2}$), 1.91 ($\mathrm{CH_2C\underline{H}_2CH_2}$), 3.04 ($\mathrm{C\underline{H}_3N^+}$), 3.29 ($\mathrm{CH_2C\underline{H}_2N^+}$) และ 3.36 ($\mathrm{CH_2C\underline{H}_2N^+}$)

C5-PIP TFSI (δ/ppm) = 0.95 ($\mathrm{C\underline{H}_3CH_2CH_2}$), 1.34 ($\mathrm{CH_3C\underline{H}_2CH_2}$), 1.41 ($\mathrm{CH_3CH_2C\underline{H}_2}$), 1.65 ($\mathrm{CH_2C\underline{H}_2CH_2}$), 1.73 ($\mathrm{CH_2C\underline{H}_2CH_2}$), 1.85 ($\mathrm{C\underline{H}_2CH_2CH_2C\underline{H}_2}$), 2.95 ($\mathrm{C\underline{H}_3N^+}$), 3.24 ($\mathrm{^+NC\underline{H}_2}$) and 3.28 ($\mathrm{C\underline{H}_2N^+C\underline{H}_2}$)

^{13}C NMR spectra

C3-PIP TFSI (δ/ppm) = 10.0 ($\mathrm{\underline{C}H_3CH_2CH_2}$), 15.1 ($\mathrm{CH_3\underline{C}H_2CH_2}$), 19.8 ($\mathrm{CH_2\underline{C}H_2CH_2}$), 47.5 ($\mathrm{\underline{C}H_3N^+}$), 61.5 ($\mathrm{CH_2\underline{C}H_2N^+}$), 65.6 ($\mathrm{CH_2\underline{C}H_2N^+}$) and 120.0 ($\mathrm{\underline{C}F_3SO_2N}$).[21]

C4-PIP TFSI (δ/ppm) = 13.5 ($\mathrm{\underline{C}H_3CH_2CH_2}$), 19.4 ($\mathrm{CH_3\underline{C}H_2CH_2}$), 19.9 ($\mathrm{CH_2C\underline{H}_2CH_2}$), 20.7 ($\mathrm{CH_2\underline{C}H_2CH_2}$), 47.4 ($\mathrm{\underline{C}H_3N^+}$), 61.3 ($\mathrm{CH_2\underline{C}H_2N^+}$), 64.2 ($\mathrm{CH_2\underline{C}H_2N^+}$) and 120.0 ($\mathrm{\underline{C}F_3SO_2N}$)

C5-PIP TFSI (δ/ppm) = 13.5 ($\mathrm{\underline{C}H_3CH_2CH_2}$), 20.1 ($\mathrm{CH_3\underline{C}H_2CH_2}$), 21.2 ($\mathrm{CH_3CH_2\underline{C}H_2}$), 21.6 ($\mathrm{CH_2\underline{C}H_2CH_2}$), 22.4 ($\mathrm{CH_2\underline{C}H_2CH_2}$), 28.5 ($\mathrm{\underline{C}H_2CH_2CH_2\underline{C}H_2}$), 48.2 ($\mathrm{\underline{C}H_3N^+}$), 61.5 ($\mathrm{^+N\underline{C}H_2}$), 118.0 ($\mathrm{C\underline{H}_2N^+C\underline{H}_2}$) and 120 ($\mathrm{\underline{C}F_3SO_2)_2N}$

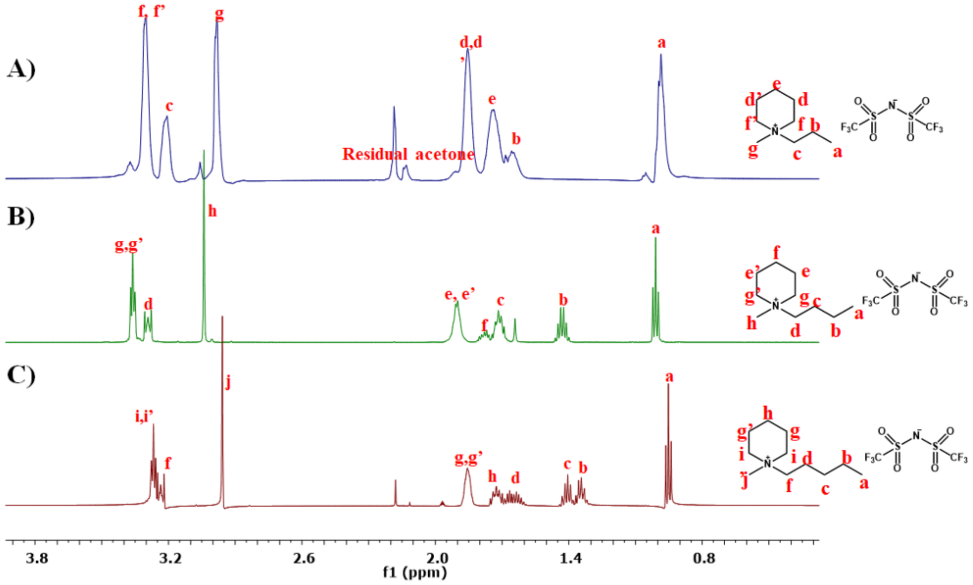

Fig. S1 ^{1}H NMR spectra of C3-PIPTFSI (A), C4-PIPTFSI (B) and C5-PIPTFSI (C).

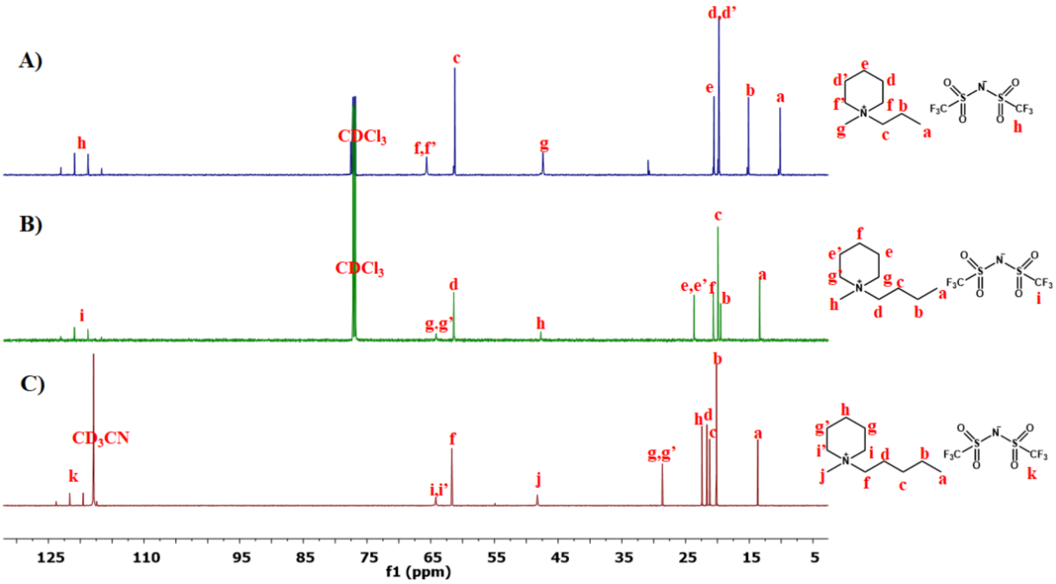

Fig. S2 ^{13}C NMR spectra of C3-PIPTFSI (A), C4-PIPTFSI (B) and C5-PIPTFSI (C).

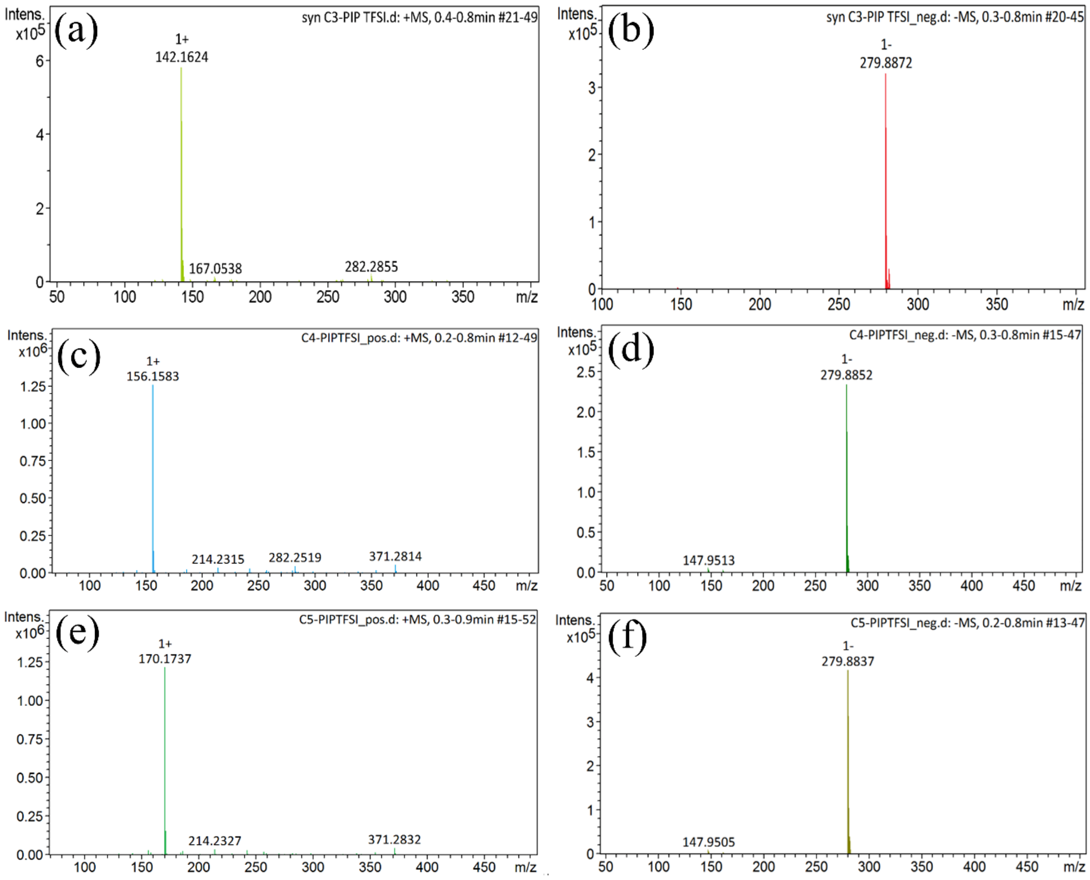

Fig. S3. APCI mass spectra of as-synthesised ionic liquids including C3-PIP (A), C4-PIP (C), C5-PIP (E) cations coupled with their TFSI anions (B, D and F, respectively).

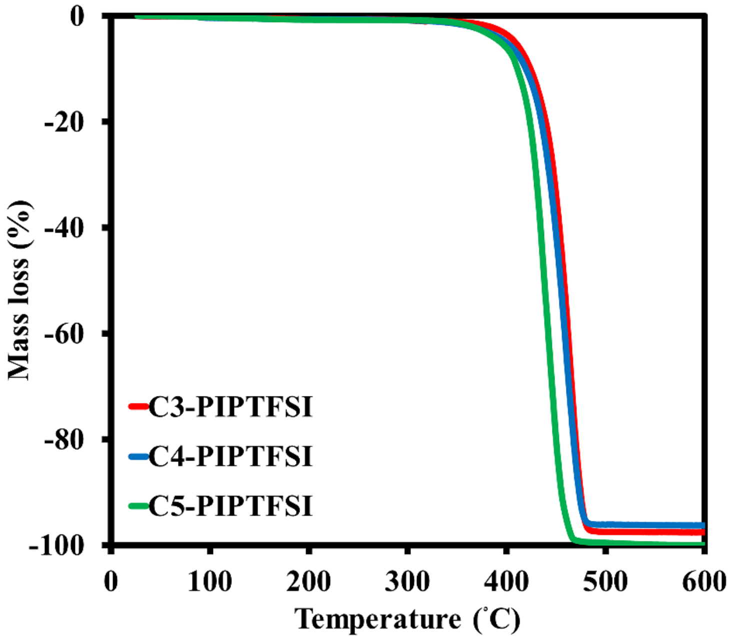

Fig. S4 TGA curves of C3-PIPTFSI, C4-PIPTFSI and C5-PIPTFSI.

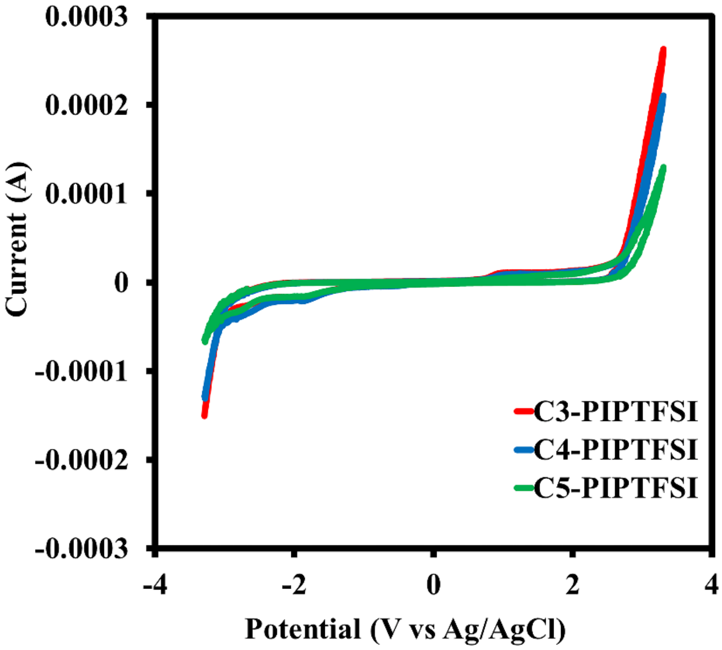

Fig. S5 Cyclic voltammograms of C3-PIPTFSI, C4-PIPTFSI and C5-PIPTFSI.

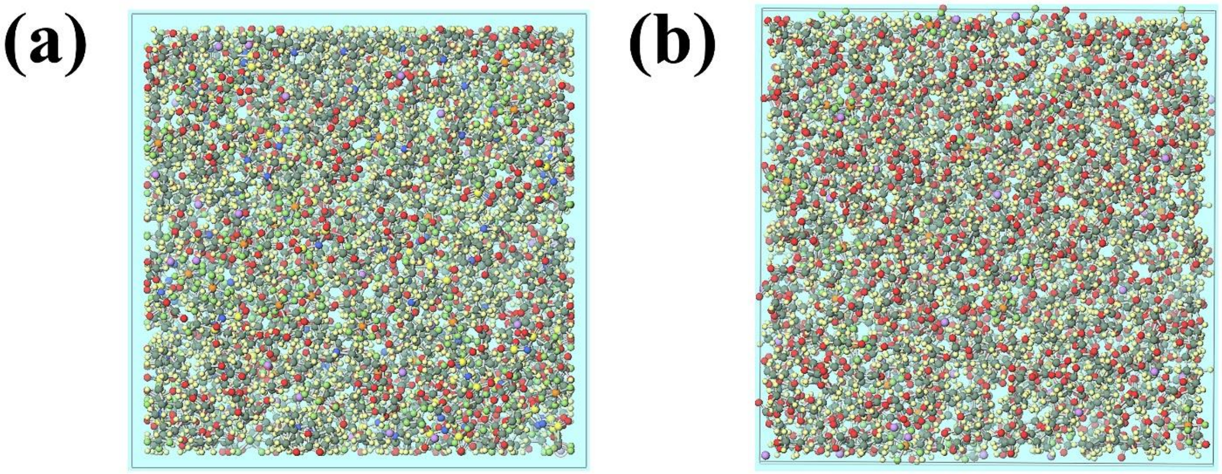

Fig. S6 Initial configuration snapshot of the simulation cell for (a) conventional electrolyte, (b) Hybrid electrolytes of piperidinium-based ionic liquids and conventional electrolyte.

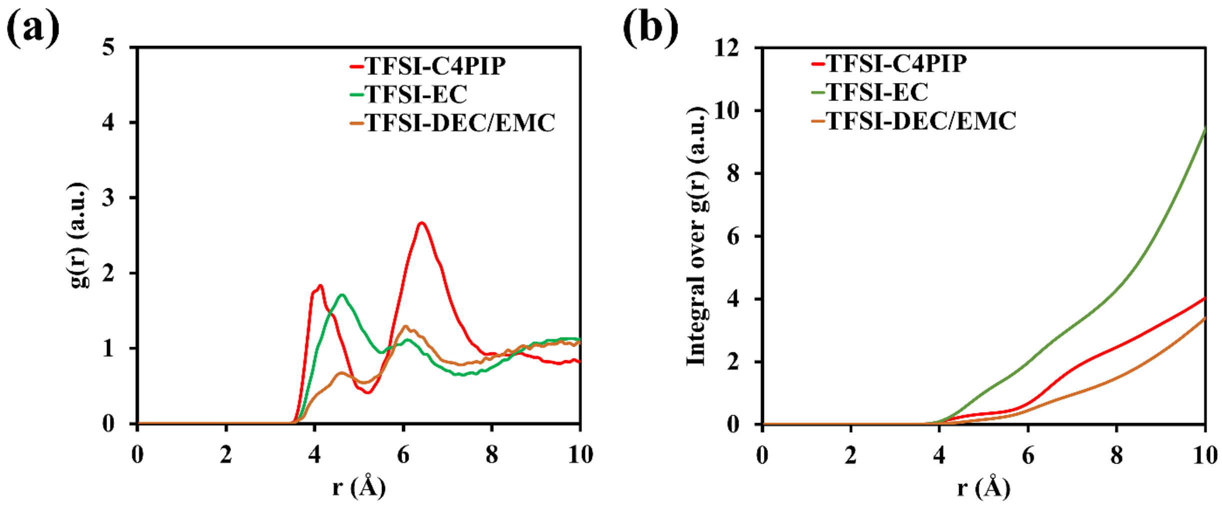

Fig. S7 Radial pair distribution function g(r) of TFSI- with C4PIP+, EC, and DEC/EMC for (a) conventional electrolyte, (b) Hybrid electrolytes of piperidinium-based ionic liquids and conventional electrolyte.

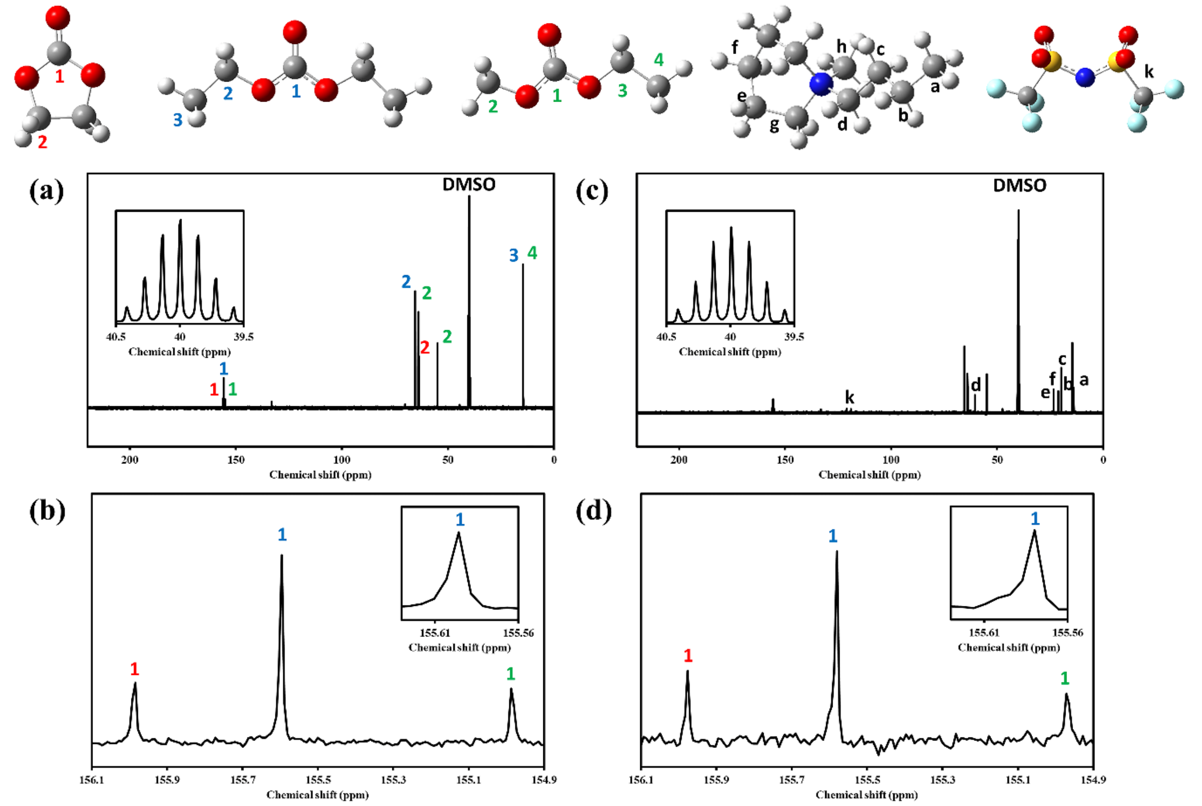

Fig. S8 ^{13}C NMR chemical shift of the commercial electrolyte (a), (b) and C4PIP-TFSI-based hybrid electrolyte (c), (d). Inset picture in both (a) and (c) are a chemical shift of DMSO. Also, inset pictures in both (b) and (d) are a chemical shift of diethyl ethylene carbonate (DEC).

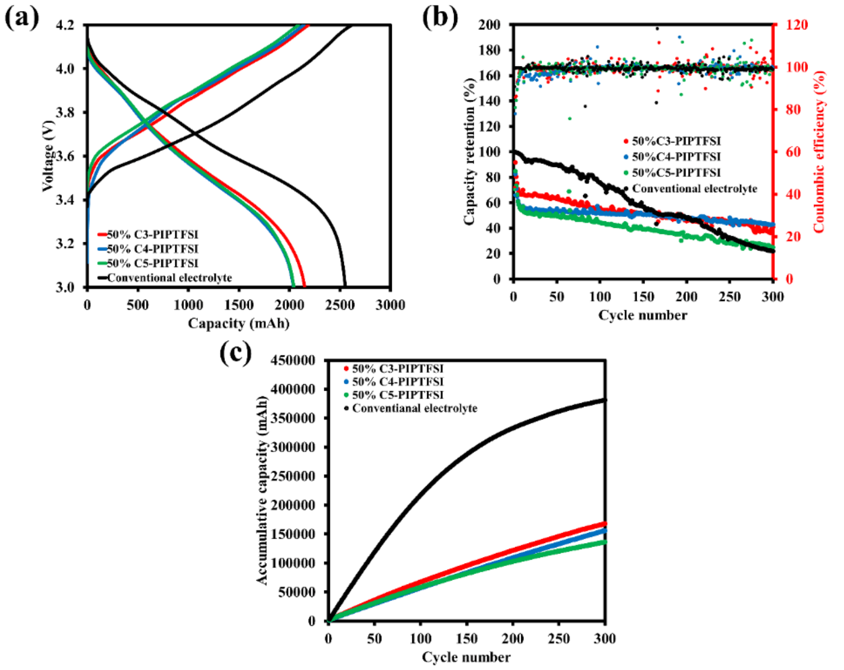

Fig. S9 Voltage profiles of the first charge-discharge process at 0.1C (a), the cycling ability at 0.5C (b), and accumulative capacity (c) of the cells using conventional and hybrid electrolytes.

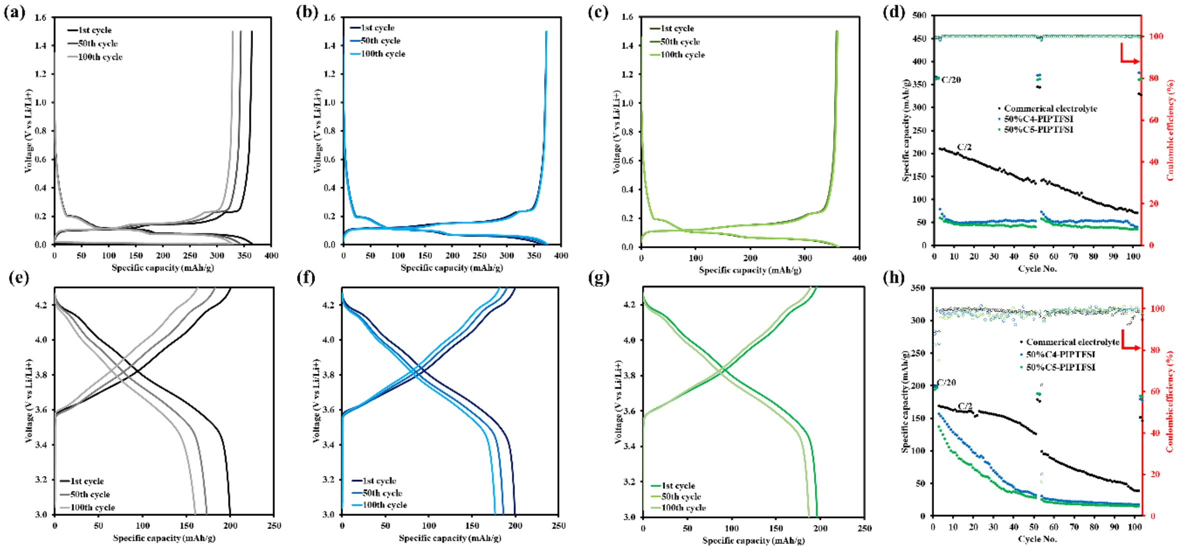

Fig. S10 Voltage profile of the 1st, 50th, and 100th charge-discharge cycles at 0.05C of (a-d) Li||graphite half-cell and (e-h) Li||NCA half-cell containing the conventional electrolyte (a and e), 50%C4-PIPTFSI hybrid electrolyte (b and f), and 50%C5-PIPTFSI hybrid electrolyte (c and g), respectively as well as the capacity retention at 0.5C of the cells using conventional and hybrid electrolytes.

Table S1. Electrochemical Stability Potential Window (ESW) of Piperidinium-based bis(trifluoromethanesulfonyl)imides (PIP-based TFSI).

Ionic liquids	Electrochemical stability window (ESW, V)			Conductivity ($mScm^{-1}$)	Density (gcm^{-3})
	Cathodic limit	Anodic limit	Overall window		
C3-PIPTFSI	-2.4	+2.4	4.8	0.65	1.40
C4-PIPTFSI	-2.4	+2.4	4.8	0.57	1.37
C5-PIPTFSI	-2.4	+2.4	4.8	0.47	1.34

Table S2. Calculated coordination number of Li-X pairs from the integration over the g(r) to 2.3 Å, total coordination number, contact ion pair (CIP) ratio, and corresponding contact ion pair formation energy (kcal mol^{-1}).

Systems	Li-Li	Li-TFSI	Li-PF6	Li-C4PIP	Li-EC	Li-DEC/DMC	Total C.N.	%CIP	%SSIP
No C4PIPTFSI-Ils	0.000	0.000	0.188	0.000	2.687	2.332	5.206	3.605	96.395
50% vol C4PIPTFSI-ILs	0.000	0.895	1.364	0.000	0.062	0.002	2.324	97.225	2.775

Table S3. Flammability test of conventional electrolyte and hybrid electrolytes.

Electrolyte	**0 second**	**30 seconds**	**40 seconds**	**Self-Extinguishing Time (SET) (s)**
1 M $LiPF_6$ in EC:DMC:DEC =1:1:1				55
50% C3-PIPTFSI			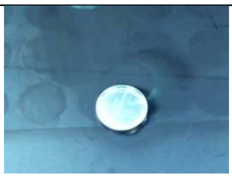	37
50% C4-PIPTFSI				32
50% C5-PIPTFSI			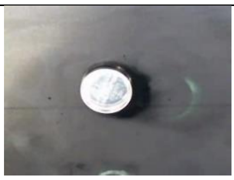	38

References

1. T. Yim, Lee, H. Y., Kim, H-J., Mun, J., Kim, S., Oh, S. M., and Kim, Y. G., *B. Korean. Chem. Soc.*, **2007**, ***28***, 1567-1572.
2. C. Maton, N. De Vos and C. V. Stevens, *Chem Soc Rev*, 2013, **42**, 5963-5977.

3. K. Machanová, A. Boisset, Z. Sedláková, M. Anouti, M. Bendová and J. Jacquemin, *Journal of Chemical & Engineering Data*, 2012, **57**, 2227-2235.
4. A. Filippov, M. Taher, F. U. Shah, S. Glavatskih and O. N. Antzutkin, *Phys Chem Chem Phys*, 2014, **16**, 26798-26805.
5. C. Y. Son, J. G. McDaniel, J. R. Schmidt, Q. Cui and A. Yethiraj, *The Journal of Physical Chemistry B*, 2016, **120**, 3560-3568.
6. M. Takeuchi, Y. Kameda, Y. Umebayashi, S. Ogawa, T. Sonoda, S.-i. Ishiguro, M. Fujita and M. Sano, *Journal of Molecular Liquids*, 2009, **148**, 99-108.
7. K. P. Jensen and W. L. Jorgensen, *Journal of Chemical Theory and Computation*, 2006, **2**, 1499-1509.
8. J. N. Canongia Lopes and A. A. H. Pádua, *The Journal of Physical Chemistry B*, 2004, **108**, 16893-16898.
9. A. D. Becke, *The Journal of Chemical Physics*, 1993, **98**, 5648-5652.
10. M. J. Frisch, G. W. Trucks, H. B. Schlegel, G. E. Scuseria, M. A. Robb, J. R. Cheeseman, G. Scalmani, V. Barone, G. A. Petersson, H. Nakatsuji, X. Li, M. Caricato, A. V. Marenich, J. Bloino, B. G. Janesko, R. Gomperts, B. Mennucci, H. P. Hratchian, J. V. Ortiz, A. F. Izmaylov, J. L. Sonnenberg, Williams, F. Ding, F. Lipparini, F. Egidi, J. Goings, B. Peng, A. Petrone, T. Henderson, D. Ranasinghe, V. G. Zakrzewski, J. Gao, N. Rega, G. Zheng, W. Liang, M. Hada, M. Ehara, K. Toyota, R. Fukuda, J. Hasegawa, M. Ishida, T. Nakajima, Y. Honda, O. Kitao, H. Nakai, T. Vreven, K. Throssell, J. A. Montgomery Jr., J. E. Peralta, F. Ogliaro, M. J. Bearpark, J. J. Heyd, E. N. Brothers, K. N. Kudin, V. N. Staroverov, T. A. Keith, R. Kobayashi, J. Normand, K. Raghavachari, A. P. Rendell, J. C. Burant, S. S. Iyengar, J. Tomasi, M. Cossi, J. M. Millam, M. Klene, C. Adamo, R. Cammi, J. W. Ochterski, R. L. Martin, K. Morokuma, O. Farkas, J. B. Foresman and D. J. Fox, *Journal*, 2016.
11. N. N. Rajput, V. Murugesan, Y. Shin, K. S. Han, K. C. Lau, J. Chen, J. Liu, L. A. Curtiss, K. T. Mueller and K. A. Persson, *Chemistry of Materials*, 2017, **29**, 3375-3379.
12. C. I. Bayly, P. Cieplak, W. Cornell and P. A. Kollman, *The Journal of Physical Chemistry*, 1993, **97**, 10269-10280.
13. L. Martínez, R. Andrade, E. G. Birgin and J. M. Martínez, *Journal of Computational Chemistry*, 2009, **30**, 2157-2164.
14. S. Nosé, *Molecular Physics*, 1984, **52**, 255-268.
15. M. J. Abraham, T. Murtola, R. Schulz, S. Páll, J. C. Smith, B. Hess and E. Lindahl, *SoftwareX*, 2015, **1-2**, 19-25.

16. S. Pronk, S. Páll, R. Schulz, P. Larsson, P. Bjelkmar, R. Apostolov, M. R. Shirts, J. C. Smith, P. M. Kasson, D. van der Spoel, B. Hess and E. Lindahl, *Bioinformatics*, 2013, **29**, 845-854.
17. B. Hess, C. Kutzner, D. van der Spoel and E. Lindahl, *Journal of Chemical Theory and Computation*, 2008, **4**, 435-447.
18. D. Van Der Spoel, E. Lindahl, B. Hess, G. Groenhof, A. E. Mark and H. J. C. Berendsen, *Journal of Computational Chemistry*, 2005, **26**, 1701-1718.
19. E. Lindahl, B. Hess and D. van der Spoel, *Molecular modeling annual*, 2001, **7**, 306-317.
20. H. J. C. Berendsen, D. van der Spoel and R. van Drunen, *Computer Physics Communications*, 1995, **91**, 43-56.
21. B. Haddad, Villemin, D., Belarbi, E-H., *J. Mater. Environ. Sci.*, 2012, **3(2)**, 312-319.